

## Electric fields of motor and frontal tDCS in a standard brain space: A computer simulation study



Ilkka Laakso<sup>a,e,\*</sup>, Satoshi Tanaka<sup>b</sup>, Marko Mikkonen<sup>a</sup>, Soichiro Koyama<sup>c,d</sup>, Norihiro Sadato<sup>c</sup>, Akimasa Hirata<sup>e</sup>

<sup>a</sup> Department of Electrical Engineering and Automation, Aalto University, Espoo, Finland

<sup>b</sup> Laboratory of Psychology, Hamamatsu University School of Medicine, Shizuoka, Japan

<sup>c</sup> Division of Cerebral Integration, National Institute for Physiological Sciences, Aichi, Japan

<sup>d</sup> School of Life Sciences, The Graduate University for Advanced Studies, Kanagawa, Japan

<sup>e</sup> Department of Computer Science and Engineering, Nagoya Institute of Technology, Nagoya, Japan

### ARTICLE INFO

#### Article history:

Received 22 February 2016

Revised 15 April 2016

Accepted 10 May 2016

Available online 14 May 2016

### ABSTRACT

The electric field produced in the brain is the main physical agent of transcranial direct current stimulation (tDCS). Inter-subject variations in the electric fields may help to explain the variability in the effects of tDCS.

Here, we use multiple-subject analysis to study the strength and variability of the group-level electric fields in the standard brain space.

Personalized anatomically-accurate models of 62 subjects were constructed from T1- and T2-weighted MRI. The finite-element method was used to computationally estimate the individual electric fields, which were registered to the standard space using surface based registration. Motor cortical and frontal tDCS were modelled for 16 electrode montages.

For each electrode montage, the group-level electric fields had a consistent strength and direction in several brain regions, which could also be located at some distance from the electrodes. In other regions, the electric fields were more variable, and thus more likely to produce variable effects in each individual. Both the anode and cathode locations affected the group-level electric fields, both directly under the electrodes and elsewhere. For motor cortical tDCS, the electric fields could be controlled at the group level by moving the electrodes. However, for frontal tDCS, the group-level electric fields were more variable, and the electrode locations had only minor effects on the group average fields.

Our results reveal the electric fields and their variability at the group level in the standard brain space, providing insights into the mechanisms of tDCS for plasticity induction. The data are useful for planning, analysing and interpreting tDCS studies.

© 2016 The Authors. Published by Elsevier Inc. This is an open access article under the CC BY-NC-ND license (<http://creativecommons.org/licenses/by-nc-nd/4.0/>).

### Introduction

Direct currents applied to electrodes attached to the intact scalp can be used to modulate brain activity (Priori et al., 1998; Nitsche and Paulus, 2000). The effects of stimulation can be altered by reversing the polarity or changing the amplitude of the current (Nitsche and Paulus, 2000; Nitsche and Paulus, 2001; Furubayashi et al., 2008). Transcranial direct current stimulation (tDCS) can modify brain plasticity, which refers to dynamic changes in the central nervous system connectivity due to normal external and internal stimuli or brain damage. Because tDCS is well tolerable and affordable (Fregni and Pascual-Leone, 2007; Hummel et al., 2008; Tanaka and Watanabe, 2009; Brunoni et al., 2012; Meron et al., 2015), it is promising as an alternative treatment strategy for diverse neurological or psychiatric diseases that

involve pathological plasticity (Kuo et al., 2014). For instance, tDCS has shown effectiveness for depression (Meron et al., 2015), chronic pain (Kuo et al., 2014), or stroke recovery (Marquez et al., 2015).

Currently, the main limitation of tDCS is the variability in its effects depending on each individual (Wiethoff et al., 2014; López-Alonso et al., 2014; Chew et al., 2015; López-Alonso et al., 2015). The underlying reason for the inter-subject variability may be that physically tDCS acts by giving rise to an electric field that polarizes the brain tissue. However, every brain is different, and the magnitude and direction of the polarizing electric field in each brain are also different. Estimating the electric fields requires numerical analysis, because the stimulating current follows a complex path between the electrodes, passing through the scalp, skull, meninges, and cerebrospinal fluid (CSF) before reaching the brain. Recently, modelling studies have shown that these anatomical features are the defining factors of the individual brain electric fields (Truong et al., 2013; Bai et al., 2014; Laakso et al., 2015; Opitz et al., 2015). The electric field is unevenly spread on the cortex, having several

\* Corresponding author at: Aalto University, Otakaari 3, 02150 Espoo, Finland.  
E-mail address: [ilkka.laakso@aalto.fi](mailto:ilkka.laakso@aalto.fi) (I. Laakso).

hotspots both under and between the electrodes (Datta et al., 2009, 2012; Bai et al., 2014; Shahid et al., 2014; Laakso et al., 2015; Saturnino et al., 2015). Because of the inter-individual variability in the electric fields, it is still not clear which of these hotspots are prevalent in a considerable portion of subjects, and which are singularities due to individual brain anatomy.

Changing the locations of the electrodes has been shown to alter the electric field in the brain (Bikson et al., 2010; Bai et al., 2014). In experiments, the effects of tDCS depend on the locations of both the stimulating and reference electrodes (Nitsche and Paulus, 2000; Nitsche et al., 2007; Bikson et al., 2010; Moliadze et al., 2010; Mehta et al., 2015), as well as their size and orientation (Ho et al., 2016). Therefore, the electrode montage could potentially be used to steer the effects of tDCS (Bai et al., 2014). However, we do not know how much the electrode montage can be used to control the electric fields in a group of subjects, or if the electric fields tend to always concentrate in the same regions despite electrode montage.

Here, we propose a systematic way to investigate the electric fields on the population level by registering individually calculated electric fields to a standard brain space. The approach helps identifying the affected brain areas in the standard space, allowing retrospective analysis of existing tDCS studies and guiding the selection of the electrode montage for future studies.

## Methods and models

### Subjects and imaging methods

All MRI scans were acquired using a 3.0 T MRI scanner (Verio; Siemens, Ltd., Erlangen, Germany). The study was approved by the local ethics committee of the National Institute for Physiological Sciences.

Structural T1-weighted MRI of 44 subjects (19–38 years, 12 female) were acquired using a Magnetization Prepared Rapid Acquisition in Gradient Echo (MPRAGE) sequence (TR/TE/TI/FA/FOV/voxel size/number of slices = 1800 ms/1.98 ms/800 ms/9°/256 mm/1.0 mm × 1.0 mm × 1.0 mm/172 to 192). In addition, T2-weighted MRI were acquired for the same subjects (TR/TE/FOV/voxel size/slice number = 4500 ms/368 ms/256 mm/1.0 mm × 1.0 mm × 1.0 mm/224 slices). Additionally, T1- and T2-weighted structural MRI of 20 male subjects (21–55 years) were obtained from a freely available repository (NAMIC: Brain Multimodality, 3.0 T MRI scanner, data and imaging parameters available online at <http://hdl.handle.net/1926/1687>). Two of the additional subjects were excluded from further analysis owing to poor image quality.

Fig. 1 shows the distribution of age, gender, ethnic group, and handedness in the study group. In total, the number of subjects was 62 (age:  $29.2 \pm 11.2$  years, 12 female).

### Cortical reconstruction and registration

Cortical surfaces were reconstructed from the MR images using the FreeSurfer image analysis software (Dale et al., 1999; Fischl et al.,

1999; Fischl and Dale, 2000; Desikan et al., 2006) (version 5.3.0, download and documentation available online at <http://surfer.nmr.mgh.harvard.edu>). The individual subjects' brain surfaces were registered using the spherical demons algorithm (Yeo et al., 2010) to a custom average template created using all 62 subjects. The effect of the registration method on the results is studied in Section 0. To present the results in the standard space, FreeSurfer was used to generate the brain surface of the Montreal Neurological Institute (MNI) ICBM 2009a nonlinear asymmetric template (Fonov et al., 2009, 2011), which was then registered with the custom template using the spherical demons algorithm. This allowed mapping of individually calculated electric fields to the MNI template brain (Fig. 2).

### Volume conductor models

T1- and T2-weighted MRI of 62 subjects were segmented using in-house software (Laakso et al., 2015) that uses FreeSurfer for brain segmentation. Briefly, tissue compartments (scalp, outer skull, inner skull, grey matter, white matter, cerebellar grey matter, cerebellar white matter, brainstem, nuclei, ventricles, and eyes) were first constructed from MR images. The compartments were further segmented based on both MR image intensities and geometrical information: the scalp compartment was segmented into skin, fat, and muscle; the skull into compact and spongy bone; and the space between the skull and grey matter into cerebrospinal fluid (CSF), blood vessels, and dura. The quality of the inner skull surface was verified slice-by-slice by visual inspection and errors were corrected when necessary. The constructed inner skull surface was used instead of the default skull strip procedure of FreeSurfer to remove dura and make sure that there was at least 0.5 mm separation between the skull and cortex. Other tissue boundaries were verified by two examiners who inspected both the 3D surface representations of tissue boundaries and a number of slices of the segmented models.

Tissue conductivities were assumed to be linear and isotropic. Measured grey matter conductivities have typically varied between 0.1–0.3 S/m in the literature (Freygang and Landau, 1955; Ranck, 1963; Stoy et al., 1982; Tay et al., 1989; Gabriel et al., 1996; Latikka et al., 2001; Akhtari et al., 2006, 2010). Therefore, the grey matter conductivity was chosen as 0.2 S/m. The white matter conductivity was assumed 30% lower than that of the grey matter (Freygang and Landau, 1955; Stoy et al., 1982; Gabriel et al., 1996). Other tissue conductivities were: blood (0.7 S/m; Gabriel et al., 1996), compact and spongy bone (0.008 and 0.027 S/m; Akhtari et al., 2002, values increased by 30% to compensate for room temperature measurements), CSF (1.8 S/m; Baumann et al., 1997), muscle (0.16 S/m; Gabriel et al., 2009), skin and fat (0.08 S/m; Gabriel et al., 2009), eye humour (1.5 S/m; Lindenblatt and Silny, 2001), and dura (0.16 S/m, same as muscle, an arbitrary choice).

The final volume conductor models were represented in a grid of cubical voxels. Fig. 3 shows a coronal slice of a volume conductor model generated using the voxel size of 0.5 mm. The voxels were assigned conductivity values differently if they were divided by a brain tissue boundary: the voxels on the boundary between the grey matter and CSF were given the average conductivity of grey matter and CSF, and similarly, the boundary between the grey and white matter was assigned the average conductivity of the grey and white matter.

Potential problems in the models were that parts of the superior sagittal or transverse sinuses were sometimes misclassified as skull, and thin structures, such as blood vessels and falx cerebri, were not necessarily continuous. The effects of these segmentation errors on the electric fields were expected to be small. To test this, we performed electric field simulations of motor cortical tDCS (anode at C3 and cathode at Fp2) in ten subjects and modified the conductivity of blood by  $\pm 20\%$ . The changes in the electric fields over the left hemisphere were at most 4% of the maximum absolute value.

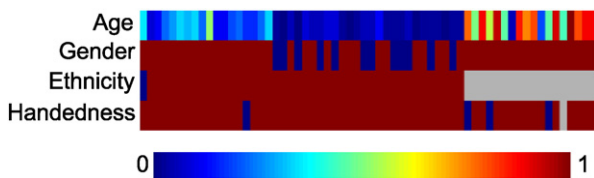


**Fig. 1.** Study population. Columns describe the data for each subject. The colour scale is normalized as following: age: 0 corresponds to 19 years and 1 corresponds to 55 years; gender: 0 = female, 1 = male; ethnicity: 0 = Caucasian, 1 = Japanese; and handedness: 0 = left, 1 = right. The data marked with grey were not available.

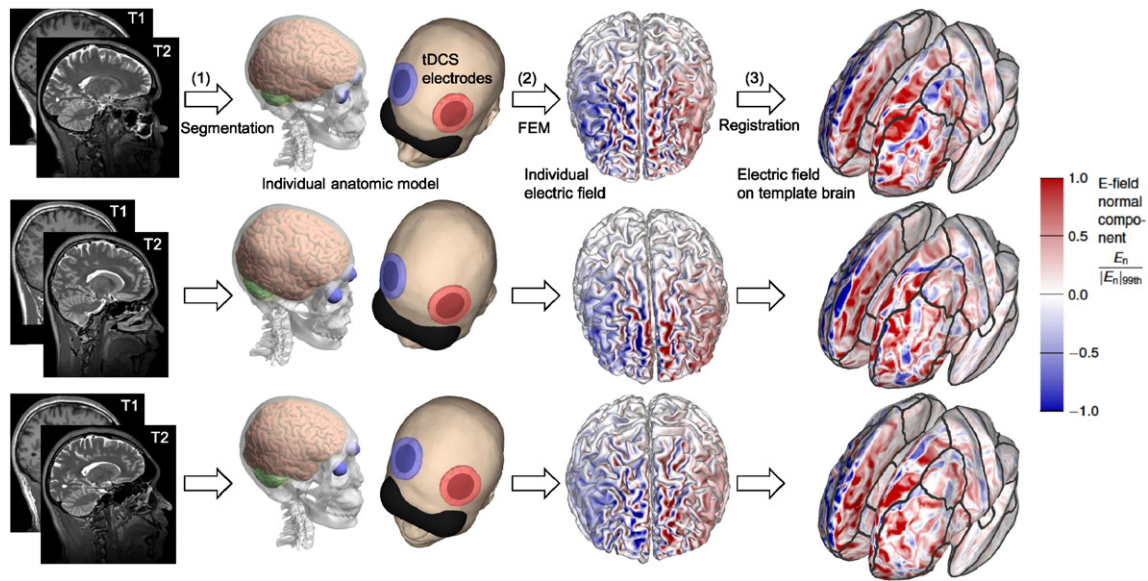


**Fig. 2.** Analysis procedure. (1) Segmentation, (2) individual electric field calculation, (3) registration to standard brain. After registration, all individual electric fields are represented in the MNI space, and can be analysed statistically. The electric fields are normalized by the 99th percentile calculated over the left hemisphere.

### Numerical electric field modelling

The electric scalar potential  $\phi$  was determined from the scalar potential equation  $\nabla \cdot \sigma \nabla \phi = -i$ , where  $\sigma$  (S/m) is the conductivity and  $i$  (A/m<sup>3</sup>) is the current source, which is nonzero only at the connector, satisfying  $\int i dV = 0$  and  $I = \frac{1}{2} \int |i| dV$  where  $I$  (A) is the stimulation current.

The equation was solved numerically using the voxels of the volume conductor model as the elements and piecewise linear basis functions, as described previously (Laakso and Hirata, 2012). The degrees of freedom were the values of the potential at the corners of each voxel. The equation system was solved to the relative residual of  $10^{-8}$ . The electric fields were calculated from the gradient of the scalar potential at each vertex of a polygonal surface located 1 mm below the grey matter surface.

Electric field simulations for one subject were run to determine the most suitable voxel size, see Supplementary note 1. Based on the results, a 0.5 mm voxel size was chosen because it gave good agreement with finer resolutions, and provided an average computational time of 40 s ( $33 \times 10^6$  elements on average) on a computer with Intel Core i7-5820K @ 3.30 GHz running Ubuntu Linux 14.04 and MATLAB R2014a.

### Electrode montages

The locations of the EEG electrodes were estimated using an automatic procedure. First, the locations of Iz, Oz, T7 and T8 in the MNI

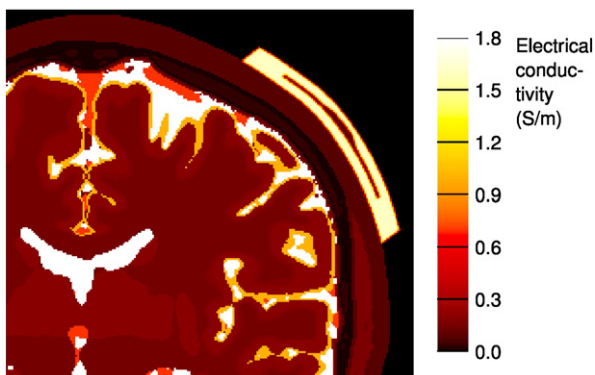


**Fig. 3.** Electrical conductivity for the voxel size of 0.5 mm.

space (Jurcak et al., 2007) were mapped to the individual subject space using an affine registration between the individual MRI and the MNI template (Johnson et al., 2007). Then, the closest points on the individual scalp surface were selected as the locations of Iz, Oz, T7 and T8. The rest of the EEG electrode locations were determined automatically from these four using the standard procedure for EEG electrode positioning (Jurcak et al., 2007).

Sixteen electrode configurations were considered for two targets, the left primary hand motor cortex, and the left dorsolateral prefrontal cortex (DLPFC). The reference locations of the anodes were over C3 and F3, respectively. The anodes were moved in anterior and posterior directions in 1 cm increments, up to  $\pm 3$  cm for C3 and up to  $\pm 2$  cm for F3. The cathode locations were either right supraorbital (Fp2), contralateral (C4 or F4), or extracephalic (monopolar stimulation). The stimulating current was 1 mA.

The electrodes were modelled based on a realistic two-compartment model proposed by Saturnino et al. (2015). They consisted of circular sponges saturated with normal saline (area 35 cm<sup>2</sup>, thickness 6 mm, conductivity 1.6 S/m). A circular 1-mm thick rubber sheet (conductivity 0.1 S/m) was inserted in the sponge, as illustrated in Fig. 4A. A connector modelled as a disk with a radius 5 mm was placed on top of the rubber sheet, serving as a current source, with a source or sink current distributed uniformly on the disk. A 1-mm bulge was added to the rubber electrode so that the connector was covered by 1 mm of rubber in every direction. As shown in Fig. 4B, the electrodes produced a current distribution with the current density maxima both directly under the connector and under the electrode edges, similarly to the findings of Saturnino et al. (2015). The electrode models were inserted into the volume conductor models by assigning each voxel a conductivity value proportional to the relative volumes of sponge and/or rubber in each voxel (see Fig. 3 for an example). For the monopolar electrode montages, the extracephalic reference electrode was modelled by a volumetric current source distributed evenly on the inferior boundary of the computation domain.

### Electric field analysis

The electric fields calculated on each individual brain surface were mapped to the MNI template brain surface using the inter-subject registration method. The resultant electric field dataset consisted of the electric field values at 277,837 vertices on the

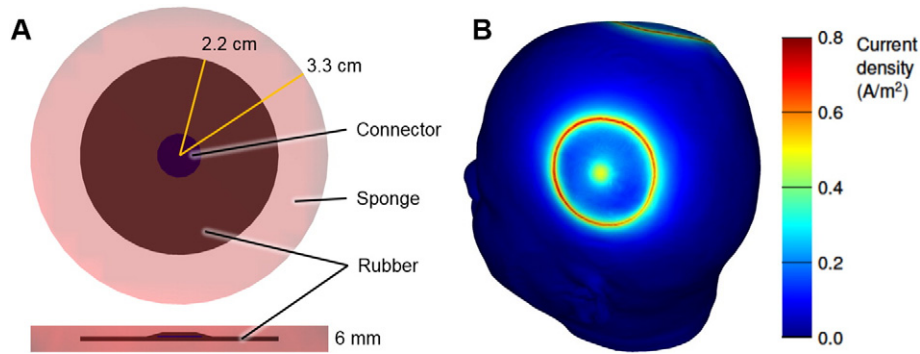


Fig. 4. Electrode models (A) and current density on a surface located 1 mm below the scalp (B).

cortical surface of the MNI template brain, for 62 subjects and 16 electrode configurations.

Electric fields perpendicular to the cortical surface can cause facilitation or inhibition of cortical activity depending on the field direction (Bindman et al., 1964). Therefore, we focused on studying the inner normal component of the electric field  $E_n$ , which can be either positive ('anodal') or negative ('cathodal'). The role of other field components (Rahman et al., 2013) is less clear because of the isotropy of horizontally oriented neurones. For completeness, we also reported the absolute value of the electric field  $|E|$ .

The sample mean value was used as the metric of the group level electric field strength and the sample standard deviation was used as the measure of variation. To compare the electric fields of different electrode montages, the change in the electric field  $\Delta E = E - E_0$  was studied by calculating the sample means of its absolute value  $|\Delta E|$  and normal component  $\Delta E_n$ . The reference electric field  $E_0$  is the electric field calculated using the C3–Fp2 or F3–Fp2 electrode montages.

## Results

### Electric fields of motor cortical tDCS

Fig. 5 shows the electric field data of motor cortical tDCS with the C3–Fp2 montage, calculated over all 62 subjects, overlaid on the inflated surface of the MNI template brain. The data of other eight motor cortical electrode montages can be found in online Supplementary material.

Several regions showed electric fields with highly consistent directions at the group level (Fig. 5E). These regions were not necessarily confined to the vicinity of the electrodes, but could also be found far from the electrodes, e.g., on the opposite hemisphere or in the medial wall. Some of the regions with consistent field directions also had a high electric field magnitude (Fig. 5A), producing anodal or cathodal electric field hotspots (Fig. 5C). One of the hotspots was in the close vicinity of the targeted hand area. Others could be found especially in sulcal pits and superficial parts of sulcal walls. At several of these hotspots, the group level electric field was dominantly in the normal direction, i.e., the normal component was larger/smaller than  $\pm|E|/\sqrt{2}$ .

The regions with a consistent field direction and high magnitude can be seen as regions with a low relative variability in Fig. 5D, e.g., near the hand knob region. However, especially frontal and parietal regions showed a large inter-subject variability, indicating that there could be high electric fields in some subjects, but in others, the fields had variable locations and/or directions. We also note that, despite small standard deviation in most of the hand knob, a small region in the dorsal/medial part showed variable electric fields due to inconsistent field directions (anodal, cathodal, or tangential) in each subject (Fig. 5E).

Compared to the normal component, the absolute value was more evenly spread and showed hotspots at several sites under and between the electrodes (Fig. 5A). Topographically, the sites with the highest

absolute value were located in gyral crowns and sulcal pits (Fig. 5E). Variability in the absolute value was smaller than that in the normal component (Fig. 5B), because it did not account for variable field directions in different subjects. Also, the variability in the absolute value did not show clear regions with a smaller or larger inter-subject variability (Fig. 5B).

Fig. 6 shows the effects of the electrode configuration on the electric field. Moving the reference electrode to the bilateral or extracephalic positions altered the electric fields within and around the hand knob region. In some regions, the changes had a consistent effect in either anodal or cathodal directions. In other regions, the changes were either in the tangential direction or the direction of the change varied between subjects. Larger changes were induced by moving the location of the stimulation electrode. Moving the anode anteriorly made the electric field in the anterior wall of the central sulcus less anodal, and moving the anode posteriorly induced opposite changes. We found that, in the case of large sponge-type electrodes studied herein, the optimal electric field in the ventral/lateral part of the hand knob was obtained when the anode was moved 2 cm posterior to C3 (Supplementary Fig. 7).

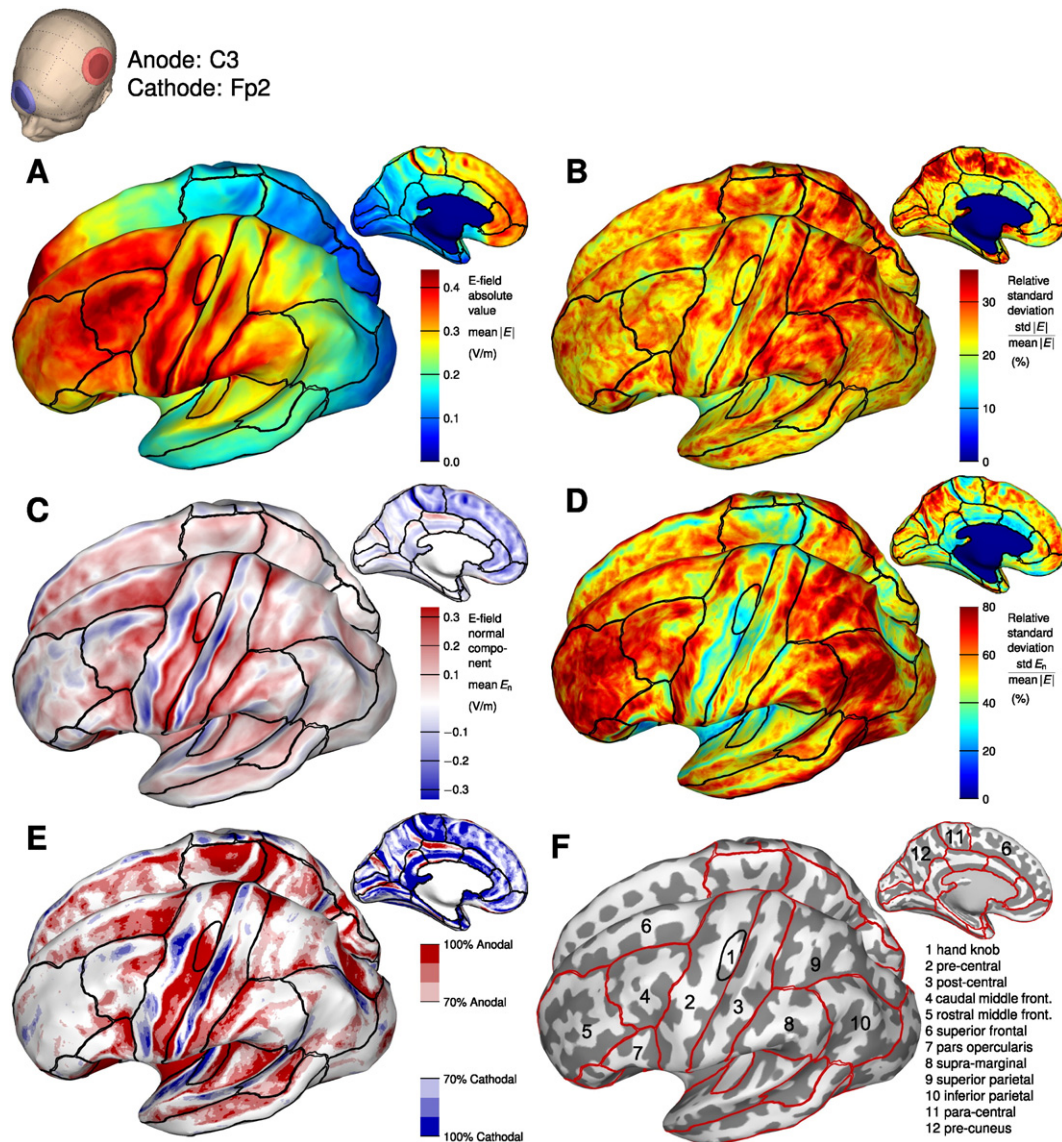
### Electric fields for tDCS of the dorsolateral prefrontal cortex

Fig. 7 shows the electric fields for the F3–Fp2 electrode montage. The data for six other DLPFC electrode montages are presented in Supplementary Figs. 11–16.

The averaging procedure revealed several regions with consistent electric field directions despite inter-subject variation (Fig. 7E). These regions were found on the lateral walls of superior frontal and middle frontal regions, and were mostly concentrated on sulcal walls facing the anode. Also notable were the consistent electric fields in the medial wall, negative on the anodal hemisphere and positive on the cathodal hemisphere. Strong electric fields reached the depth of the cingulate sulcus.

Comparison of Figs. 5D and 7D indicated that the relative standard deviation of the electric field was larger for frontal tDCS than for motor cortical tDCS. Whereas motor cortical tDCS had a low-variability high-field region under the anode, no similar region was visible for frontal tDCS. The higher degree of variability was due to more variable field directions, because the variation in the magnitude of the electric field was comparable to that of motor cortical tDCS (Figs. 5B and 7B).

Fig. 8 shows the effect of the electrode locations on the electric fields. Changing the reference electrode location to the bilateral location only had a minor impact on the electric fields. In contrast, changing to an extracephalic reference electrode reduced the overall field magnitude (see Supplementary Fig. 12). Moving the anode had inconsistent effects on the electric field depending on each individual. As the result, while the absolute changes in the electric field were of similar magnitude to those for motor cortical tDCS, the normal component changed little, especially compared to the higher inter-subject variability (Fig. 5D).



**Fig. 5.** Mean electric fields and their variability for motor cortical tDCS calculated over 62 subjects. The anode is located at C3 and the cathode over contralateral supraorbital (Fp2). A, B: The mean value of the electric field absolute value and its standard deviation. C, D: The mean value of the electric field normal component and its standard deviation. E: The distribution of the normal component direction among the subjects. High or low values indicate that the field directions are consistently anodal or cathodal at the group level. F: Cortical folding pattern and parcellation produced by FreeSurfer. Insets show the results on the medial wall of the left hemisphere. Colour scales are truncated at the 99th percentile.

### Robustness

#### Group size

The effect of the group size on the group-level electric fields was studied using Monte Carlo simulations. Two non-intersecting groups of equal size were selected randomly from among the 62 subjects and the correlations in the group electric field data were calculated. The process was repeated 500 times for each group size, and the sample mean and standard deviation of the correlation were calculated. Fig. 9 shows the correlations in the group-level electric fields calculated over the whole left hemisphere and over the left hand knob region for the C3–Fp2 electrode montage. The correlations in the absolute value are stronger than those in the normal component, indicating that a larger number of subjects is needed for investigating the field with directional information. For the normal component, the correlation reaches  $r = 0.90$  for a group size of 13 and  $r = 0.95$  for a group size of 26. For the absolute value, similar correlations can be obtained with groups of three and seven subjects, respectively. A much larger number

of subjects is needed to reliably estimate the standard deviation of the electric field: 22 subjects for  $r = 0.90$  and approximately 44 subjects for  $r = 0.95$  (extrapolated).

#### Inter-subject registration

To investigate the effect of the registration method on the group-level electric field data, four different surface-based registration methods were applied for the same data. The methods were the following: FreeSurfer (Fischl et al., 1999) with the default FS40 template, FreeSurfer with a custom template, the spherical demons algorithm (Yeo et al., 2010) with the example atlas constructed from 39 subjects (DW Atlas 1 to 39), and the spherical demons algorithm with a custom template. The custom templates were generated from all 62 subjects using the respective algorithms for registration (Klein et al., 2010).

Fig. 10 shows the distribution of the electric field directions determined using each registration method. Despite slight differences, all four registration methods produced qualitatively similar results, identifying the same regions with a low variability in the field direction. We

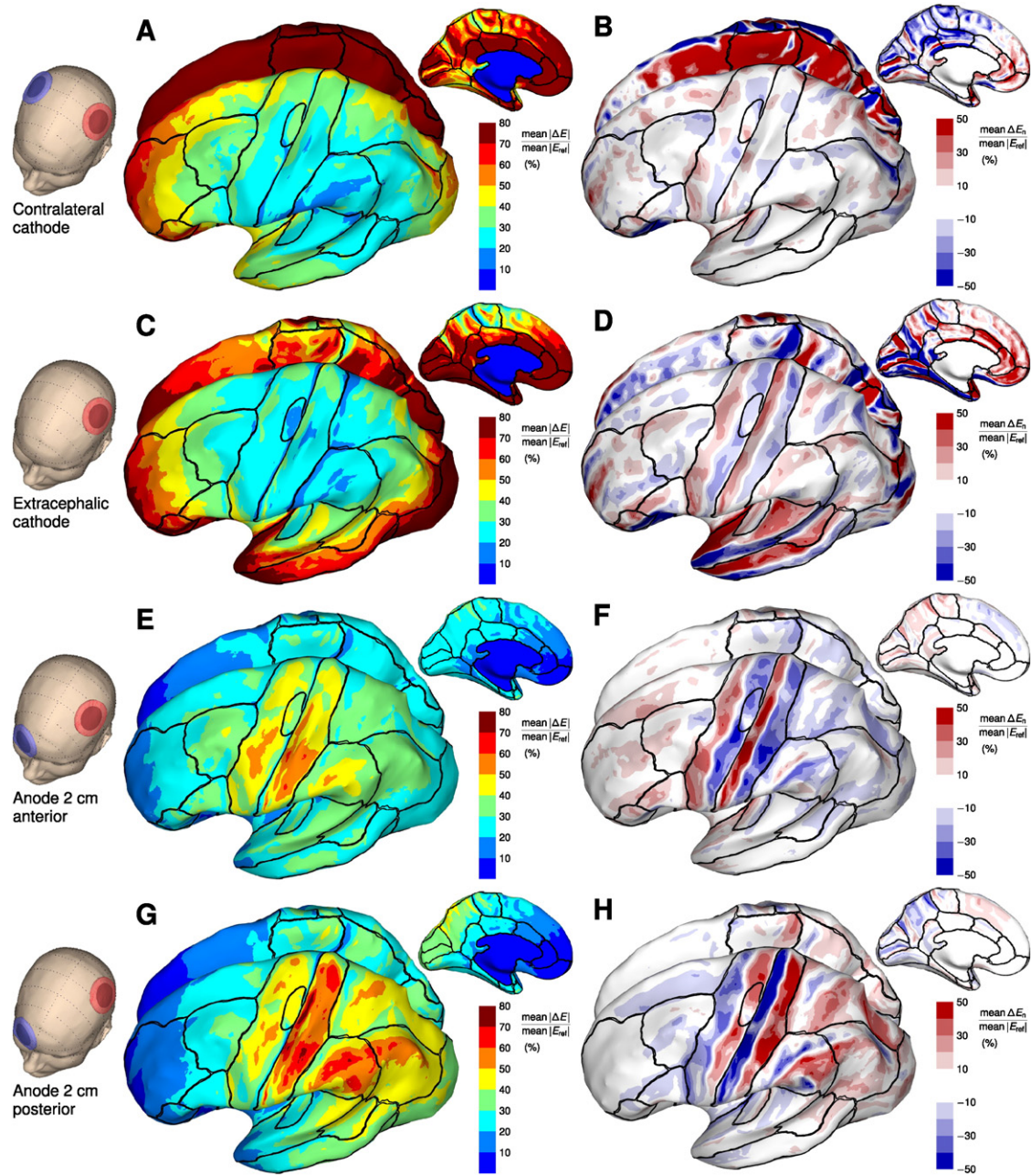


**Fig. 6.** Differences in mean electric fields due to electrode locations for the motor cortical target. The electric fields of (A, B) C3–C4, (C, D) monopolar C3, (E, F) anode 2 cm anterior to C3, and (G, H) anode 2 cm posterior to C3 are compared to the electric fields of the C3–Fp2 montage. The left column shows the mean difference in the electric field and the right column shows the mean difference in the normal component. The values are normalized by the mean absolute value of the electric field for the C3–Fp2 montage (Fig. 5A).

chose to use the spherical demons algorithm with a custom template, because using a study-specific template has been previously shown to improve the registration quality compared to generic templates (Klein et al., 2010; Winkler et al., 2012).

## Discussion

The prime novelty compared to previous computer simulation studies is that our approach allows investigation of the electric fields on the population level. Simulations in 62 subjects and surface-based registration allowed us to construct a surface-based “atlas” of likely areas affected by tDCS, without a need to take into account the singularities of individual brain anatomy. The results can be presented in the standard

brain space, which allows relating the electric fields with neuroimaging data or anatomical or functional atlases (Van Essen and Dierker, 2007).

### Regions with positive and negative electric fields

The results showed that there are brain regions where the electric fields are oriented similarly and are consistently strong among the population. Another class of regions consisted of high-variability regions where the electric fields could be strong depending on the individual, but at the group level, the fields had variable strengths and/or directions. Both the low- and high-variability regions with strong electric fields are potential sources of physiological effects of tDCS. We hypothesize that the modulation of high-variability regions causes effects that

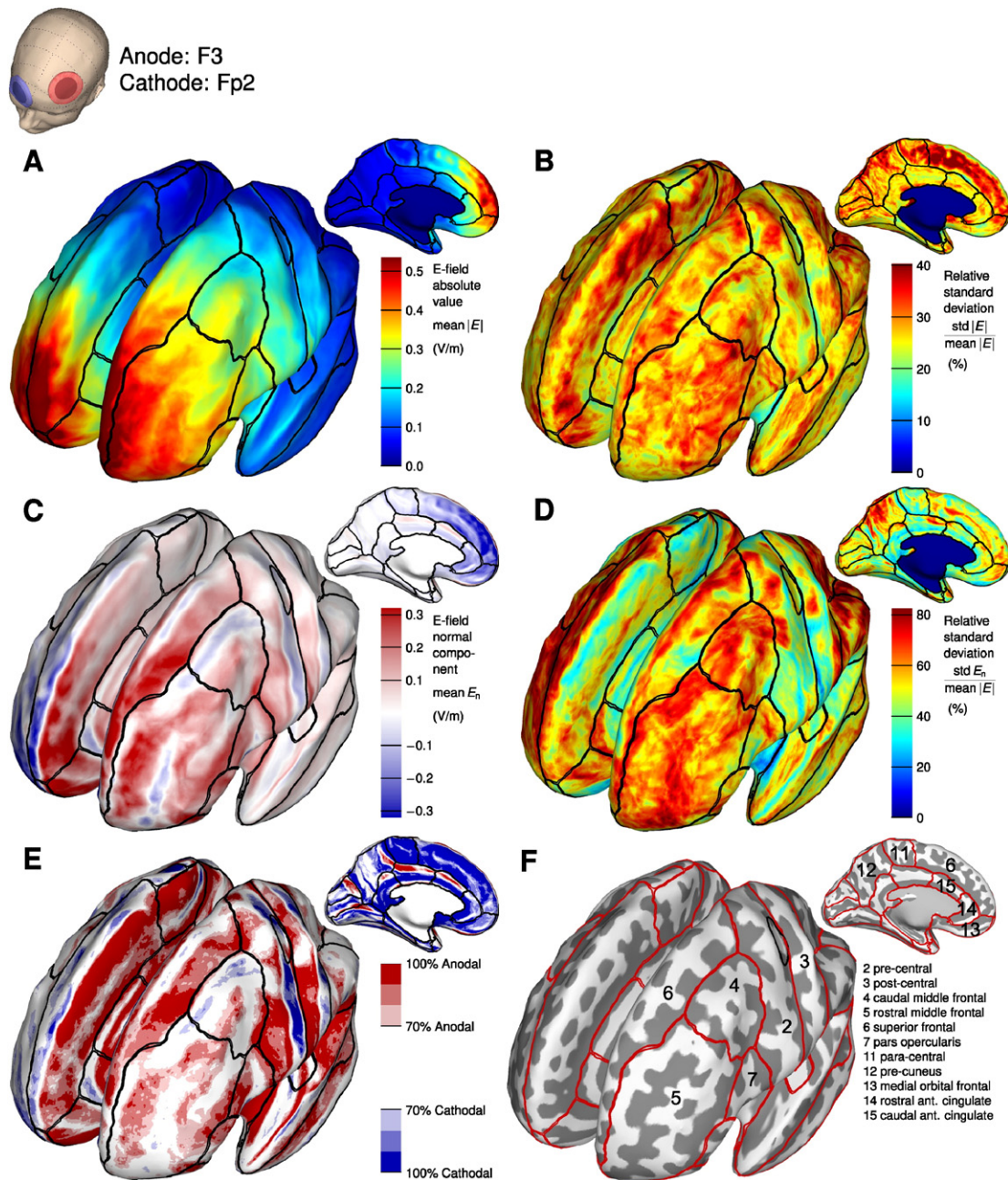


**Fig. 7.** Electric fields for DLPFC stimulation. The anode is located at F3 and the cathode over the contralateral supraorbital (Fp2). A, B: The mean value of the electric field absolute value and its standard deviation. C, D: The mean value of the electric field normal component and its standard deviation. E: The distribution of the normal component direction among the subjects. High or low values indicate that the field directions are consistently anodal or cathodal at the group level. F: Cortical folding pattern and parcellation produced by FreeSurfer. Insets show the results on the medial wall of the left hemisphere. Colour scales are truncated at the 99th percentile.

are likely to be variable in a group of subjects, and could be one of the origins of the variability in tDCS. Oppositely, a statistical analysis of a hypothetical tDCS study would only detect effects that are similar in multiple subjects and more likely to originate from the low-variability regions.

For motor cortical tDCS with a contralateral frontopolar cathode, the electric fields were strong and directed consistently into the cortex in the anterior wall of the central sulcus (Brodmann area BA4) near the hand knob region. This finding is similar to our previous study, where we observed concentration of electric fields in the hand motor area (Laakso et al., 2015). However, in the dorsal/medial part of the hand knob, the field directions were variable between subjects, which we attribute to anatomical variations in the shape of the hand knob: depending

on the individual hand knob anatomy, the current may enter the hand knob laterally and exit medially, enter the cortex uniformly over the whole hand knob region, or flow tangentially following the course of the central sulcus.

In addition to the hand knob, there were several other regions with a high mean electric field and low variability. For instance, strong electric fields comparable to those in the hand knob region could be found in the premotor areas (BA6), the fundus of the central sulcus (BA3a), the postcentral gyrus (BA1), and the postcentral sulcus (BA2). These stimulation hotspots are not artefacts, but features that are common for a considerable portion of subjects, i.e., tDCS typically induces electric fields in these areas. Thus, they could play a part in the mechanisms of tDCS.

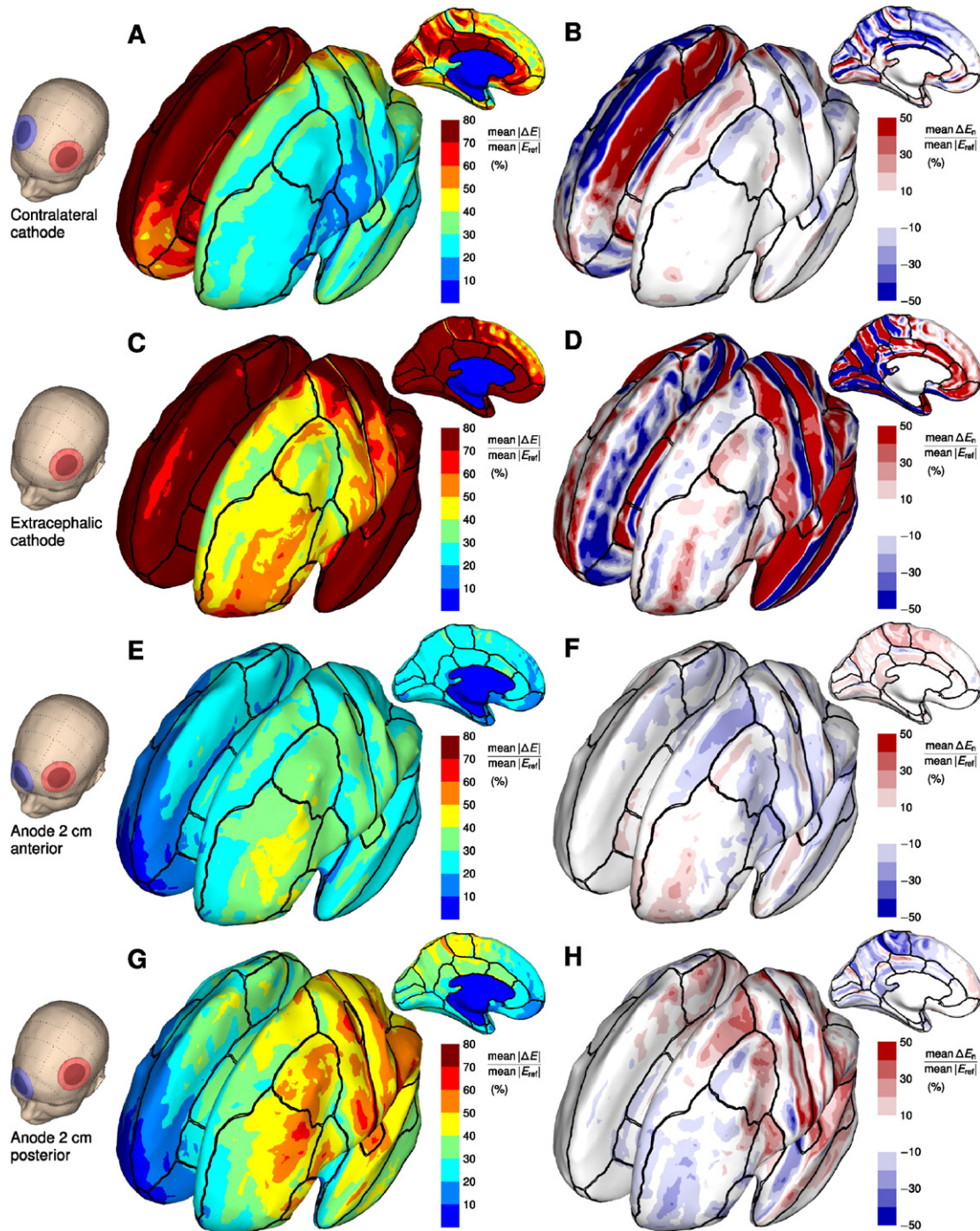


**Fig. 8.** Differences in mean electric fields due to electrode montage for frontal tDCS. The electric fields of (A, B) F3–F4, (C, D) monopolar F3, (E, F) anode 2 cm anterior to F3, and (G, H) anode 2 cm posterior to F3 are compared to the electric fields of the F3–Fp2 montage. The left column shows the mean difference in the electric field and the right column shows the mean difference in the normal component. The values are normalized by the mean absolute value of the electric field for the F3–Fp2 montage (Fig. 7A).

We note that, even directly under the anode, the electric field direction can be consistently cathodal, i.e., out of grey matter. The phenomenon is visible both in individual (Fig. 2) and group electric field data (Fig. 5E). It occurs when the current enters and leaves a gyrus at opposite sites. Examples are the anterior walls of the post-central (BA3b) and pre-central gyri (BA6) for motor cortical tDCS (Fig. 5). Although not visible in the figures, there were also consistently cathodal electric fields on the ceiling of the lateral sulcus, near the location of the secondary somatosensory cortex.

For frontal tDCS, the electric fields were more variable than for motor cortical tDCS. Still, strong consistently anodal electric fields

were found in the lateral walls of the superior frontal and middle frontal gyri (BA9 and BA46). These sites are in agreement with the data from two subjects in a previous study (Bai et al., 2014). The electric fields were most consistent on the walls of the interhemispheric fissure, negative on the anodal hemisphere, and positive on the opposite hemisphere. Contrary to motor cortical tDCS, there were no areas with consistently negative electric fields under the anode, even though such areas existed in individual subjects (Fig. 2). The larger variability in the individual electric fields may be important for explaining the variable effectiveness of frontal tDCS (Tremblay et al., 2014).

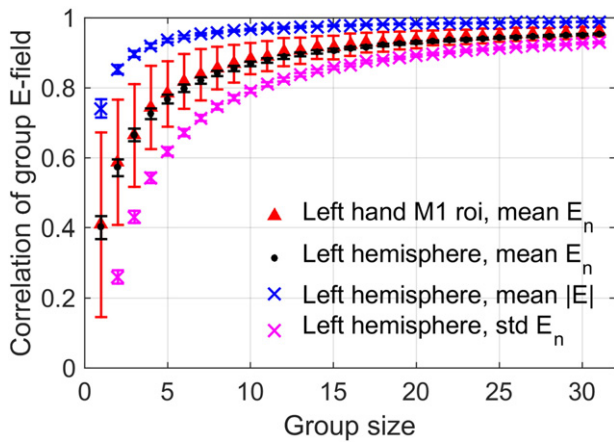


**Fig. 9.** Effect of group size on the group electric field data for the C3–Fp2 electrode montage. The mean electric field normal component, mean absolute value, and standard deviation were calculated for two groups of equal size in the whole left hemisphere and in the hand knob region. Correlations in the vertex-wise data were calculated between 500 randomly selected pairs for each group size (mean  $\pm$  standard deviation).

#### Group effects of electrode montage

Moving the anode  $\pm 2$  cm in the anterior–posterior direction altered the mean electric field in the hand M1 by up to  $\pm 40\%$ . We note that there were some subjects whose electric fields changed very little or oppositely compared to the group average. In experimental work, the anode is typically located at the hotspot identified using transcranial magnetic stimulation (TMS). However, previous studies have shown that the TMS hotspot may be shifted anteriorly compared to the anatomical location of the hand knob or C3 (Diekhoff et al., 2011; Sparing et al., 2008). Here, we found that an anterior location of anode may reduce the electric field, and thus, the anode should be placed posteriorly for optimal stimulation of the motor cortex. When using a paired montage of two large electrodes with the cathode over the contralateral orbit, the optimal anode location for targeting the anterior wall of the central sulcus was 2 cm posterior to C3.

The sensitivity of the group-level electric fields to the displacement of the anode is advantageous on one hand, because it indicates that stimulation can be optimized or targeted at the group level by moving the electrodes. On the other hand, the effects of the stimulating electrode location may have important implications on studies of intra-individual variability of tDCS (Chew et al., 2015; López-Alonso et al.,

2015). If a 1 cm difference produces a 20% change in the brain electric fields, and possibly more in individual subjects, accurately controlling the electrode placement between tDCS sessions is essential for controlling intra-subject variability. We note that an earlier study showed only minor effects of electrode displacement in two subjects (Bai et al., 2014), possibly because the electric fields were averaged over a larger region.

Moving the reference electrode to the contralateral M1 or to an extracephalic position altered the electric field in the left M1 and other regions. Depending on the montage and region, the fields could either increase or decrease. Experimental studies have observed variations in the effects of tDCS depending on the reference electrode location. For instance, monopolar tDCS has a decreased effectiveness compared to a frontopolar reference (Moliadze et al., 2010). Our results suggest that this may be due to a decreased (approximately 10–20%) mean electric field in the primary motor cortex in the anterior wall of the central sulcus.

A few studies have observed differential effects of unilateral and bilateral tDCS (Lindenberg et al., 2013; Sehm et al., 2013). Here, there were only relatively small differences in the electric fields in the hand M1 for unilateral and bilateral electrode montages. Therefore, differential physiological effects, such as inter-hemispheric inhibition (Curtis, 1940), are most likely due to simultaneous stimulation of the bilateral M1. However, we cannot exclude the possibility of contributions from other regions with high electric fields (Fig. 6). Interestingly, there were large differences in the electric fields on the medial wall, where bilateral tDCS has shown enhanced connectivity compared to unilateral tDCS (Lindenberg et al., 2013).

For frontal tDCS, the electric fields were more variable, which we attribute to the larger variability in the cortical folding pattern in the frontal regions. It was also difficult to manipulate these fields at the group level by changing the electrode configuration. Even though the electrode configuration affected the individual electric fields, the mean electric fields did not show large changes because, as the field decreased in some subjects, in others it increased. Thus, the electric fields cannot be easily controlled at the group level using large electrodes as considered herein.

High-variability regions identified in this study cannot be consistently stimulated at the group level using traditional tDCS electrode montages that consist of a pair of large electrodes. For targeting these regions, alternative approaches are needed. For instance, personalized electrode optimization methods could be used to remove inter-subject variability (Dmochowski et al., 2011; Sadleir et al., 2012; Ruffini et al., 2014). These approaches use individual electric field simulations to

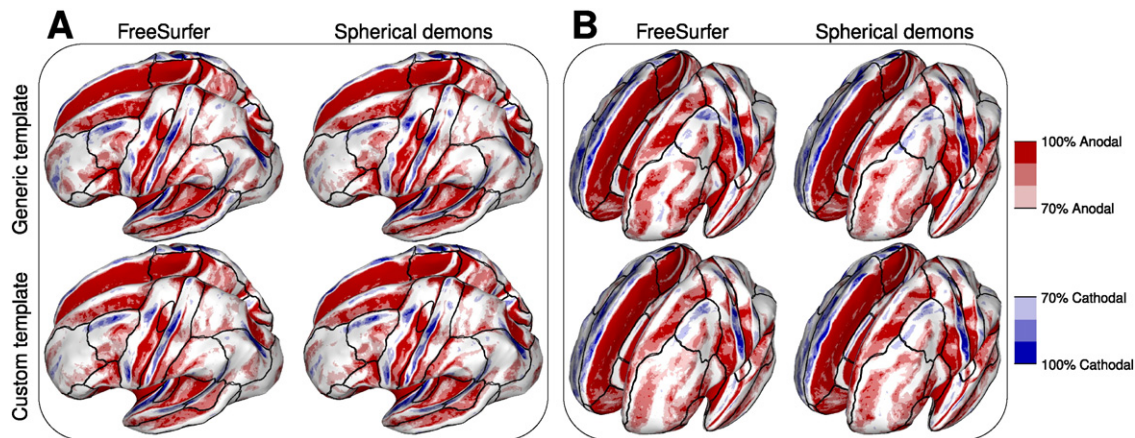


**Fig. 10.** Comparison of four surface-based registration methods. The registered electric field directions are shown for bilateral tDCS of the motor cortex (A) and DLPFC (B). The electrode montages are C3–C4 and F3–F4, respectively. Each registration method produces consistent field directions in the same regions. Differences between the registration methods can be seen in e.g. parietal and frontal areas.

design an electrode montage that produces a desired electric field in the targeted area and minimizes the electric field in non-target regions. Another possibility would be to design electrode montages that minimize the variability at the group level. For instance, here we found that the medial part of the hand knob, which showed a large variability, could be targeted by moving the anode 3 cm posteriorly (Supplementary Fig. 9). However, none of the studied montages could reduce the variability in the DLPFC. It remains future work to study whether the variability in the group-level electric fields could be reduced by using smaller electrodes or electrode montages that feature multiple electrodes, such as high-definition tDCS (Minhas et al., 2010; Kuo et al., 2013).

#### Mechanisms of tDCS

Our results suggest that if tDCS produces strong enough electric fields to affect one area in a group of subjects, e.g. the hand M1, it would also affect several other regions at the group level simultaneously, either with anodal or cathodal field directions. The electric field magnitudes peaked at around 0.5 V/m, which is comparable to experimentally measured thresholds for modulation of neuronal activity (Bindman et al., 1964; Francis et al., 2003).

tDCS can induce changes in a variety of regions also distant from the electrodes (Lang et al., 2005), and alter intra- and interhemispheric connectivity between brain areas (Polanía et al., 2011a, b; Lindenberg et al., 2013; Sehm et al., 2013). One potential hypothesis is that tDCS affects an area directly under the electrode, inducing local changes that manifest itself in increased or decreased connectivity to other regions, leading to functional changes that are more widespread than the stimulated area only. In view of our results, spatial spread of tDCS and alterations in connectivity may as well be related to simultaneous facilitation/inhibition of multiple separate areas. If this is the case, relating electric fields to the effects of tDCS requires analysis that must consider functional interactions in addition to local electric field values.

There is evidence of non-linearity or non-monotonicity in responses to tDCS, the effects reversing at higher current magnitudes (Batsikadze et al., 2013). Possible individual differences in the responses to different stimulation current intensities have also been reported (Chew et al., 2015). We hypothesize that these effects are either due to local effects of electric fields, i.e., in each affected region, the response is a non-linear function of the local electric field; or they are of global nature, i.e., as the current magnitude increases, more brain areas become affected, among them areas with either anodal or cathodal field directions.

The network effects of stimulation and potential non-linearity have so far been studied using large electrodes. However, as shown here, these types of electrodes produce widespread electric fields with many potential loci of stimulation, not only in individuals but also at the group level. More focal tDCS techniques that use multiple smaller electrodes (Kuo et al., 2013; Miranda et al., 2013; Ruffini et al., 2014) could be used to study whether the underlying mechanisms are due to local or widespread modulation of cortical activity.

#### Limitations

Because our approach requires mapping the electric fields to a common template, it is affected by the quality of the inter-subject registration. We found that different registration methods identified the same low-variability regions, and none of the methods provided systematically smaller variability than the others. The methods produced slightly different results in e.g. frontal regions, which also showed a high variability in the electric fields. Therefore, some of the variability in these regions may originate from errors in the registration procedure. However, we note that all variability in the electric fields is due to anatomical factors, and is thus expected to be larger in regions with a larger anatomical variability, e.g., in frontal regions, which have complex cortical folding patterns. Lastly, even if all anatomical landmarks were registered

perfectly, the same might not be true for functional regions, which could be located in different anatomical locations in different individuals.

The tissue DC conductivity values are an important uncertainty factor. In our results, the electric field magnitudes were higher than those in previous studies (Datta et al., 2012; Truong et al., 2013; Miranda et al., 2013; Bai et al., 2014), mainly because we assumed a lower conductivity for the scalp. Previous work has shown that decreasing the scalp conductivity to 25% increases the magnitude of the brain electric fields by about 70%, but has only minor effects on their spatial distribution (Laakso et al., 2015; Saturnino et al., 2015). There were also differences in other conductivity values, including those of the brain. For instance, the grey matter conductivity has typically been chosen to be 0.33 S/m or 0.276 S/m, as derived from the literature data by Hauelsen et al. (1997) and Wagner et al. (2004). Inter-individual variations in brain conductivity have also been reported (Akhtari et al., 2006, 2010). Such variations could alter individual electric fields but are unlikely to affect the group-level electric field data presented herein. An additional uncertainty factor is that we did not model the electrical anisotropy of white matter (Suh et al., 2012; Shahid et al., 2014; Wagner et al., 2014). However, the effect of anisotropy on the electric field is expected to be smaller in the cortical grey matter than deep inside white matter (Suh et al., 2012; Shahid et al., 2014; Wagner et al., 2014).

Lastly, we note that the results presented herein are only valid for paired montages of large electrodes, which are the most commonly used configurations for tDCS (Nitsche et al., 2008). However, our inter-subject registration and averaging approach can be used without modifications to study other kinds of electrode montages as well.

#### Conclusion

We proposed a method for studying the electric fields of tDCS on the group level. The approach allows investigation of areas affected by tDCS in a standard brain space, and with minor modifications is also applicable to other transcranial electrical neuromodulation techniques, including transcranial alternating current stimulation and random noise stimulation.

Several brain regions had consistently strong electric fields in the population and are potential sources of the effects of tDCS. There exist both regions where the group-level electric fields are consistently anodal or cathodal, depending on the electrode montage, as well as regions with a high inter-subject variability in the electric field directions. The question as to whether simultaneous modulation of multiple areas contributes to tDCS-induced plasticity needs to be further explored. For this purpose, the approach presented here could be used to design focal tDCS techniques that minimize the spatial spread and variability of the group-level electric fields. The group-level electric field magnitudes can be estimated using only a few subjects, but investigating the field directions and variability may require more than 20 individual models (Fig. 9).

We observed effects of the stimulating and reference electrode locations not only on the individual but also on the group-level electric fields. Therefore, the electrode locations must be accurately controlled for reducing both inter-study and intra-subject variability. Lastly, the electric fields of frontal tDCS were highly variable and could not be controlled at the group level by moving the electrode locations. We expect that frontal tDCS will produce variable results unless the electric fields are controlled using individual modelling and/or new kinds of electrode montages.

#### Acknowledgements

This study was supported by funding from the Japan Society for the Promotion of Science (JSPS KAKENHI, grant nos. 24680061 and 16H03201).

## Appendix A. Supplementary data

Supplementary data to this article can be found online at <http://dx.doi.org/10.1016/j.neuroimage.2016.05.032>.

## References

- Akhtari, M., Bryant, H.C., Mamelak, A.N., Flynn, E.R., Heller, L., Shih, J.J., Mandelkern, M., Matlachov, A., Ranken, D.M., Best, E.D., DiMauro, M.A., Lee, R.R., Sutherling, W.W., 2002. Conductivities of three-layer live human skull. *Brain Topogr.* 14 (3), 151–167.
- Akhtari, M., Salamon, N., Duncan, R., Fried, I., Mathern, G.W., 2006. Electrical conductivities of the freshly excised cerebral cortex in epilepsy surgery patients; correlation with pathology, seizure duration, and diffusion tensor imaging. *Brain Topogr.* 18 (4), 281–290.
- Akhtari, M., Mandelkern, M., Bui, D., Salamon, N., Vinters, H.V., Mathern, G.W., 2010. Variable anisotropic brain electrical conductivities in epileptogenic foci. *Brain Topogr.* 23 (3), 292–300.
- Bai, S., Dokos, S., Ho, K.A., Loo, C., 2014. A computational modelling study of transcranial direct current stimulation montages used in depression. *NeuroImage* 87, 332–344.
- Batsikadze, G., Moliadze, V., Paulus, W., Kuo, M.F., Nitsche, M.A., 2013. Partially non-linear stimulation intensity-dependent effects of direct current stimulation on motor cortex excitability in humans. *J. Physiol. Lond.* 591 (Pt 7), 1987–2000.
- Baumann, S., Wozny, D., Kelly, S., Meno, F., 1997. The electrical conductivity of human cerebrospinal fluid at body temperature. *IEEE Trans. Biomed. Eng.* 44 (3), 220–223.
- Bikson, M., Datta, A., Rahman, A., Scaturro, J., 2010. Electrode montages for tDCS and weak transcranial electrical stimulation: role of “return” electrode’s position and size. *Clin. Neurophysiol.* 121 (12), 1976–1978.
- Bindman, L.J., Lippold, O.C., Redfearn, J.W., 1964. The action of brief polarizing currents on the cerebral cortex of the rat (1) during current flow and (2) in the production of long-lasting after-effects. *J. Physiol.* 172, 369–382.
- Brunoni, A.R., Nitsche, M.A., Bolognini, N., Bikson, M., Wagner, T., Merabet, L., Edwards, D.J., Valero-Cabre, A., Rotenberg, A., Pascual-Leone, A., Ferrucci, R., Priori, A., Boggio, P.S., Fregni, F., 2012. Clinical research with transcranial direct current stimulation (tDCS): challenges and future directions. *Brain Stimul.* 5 (3), 175–195.
- Chew, T., Ho, K.A., Loo, C.K., 2015. Inter- and intra-individual variability in response to transcranial direct current stimulation (tDCS) at varying current intensities. *Brain Stimul.* 8 (6), 1130–1137. <http://dx.doi.org/10.1016/j.brs.2015.07.031>.
- Curtis, H.J., 1940. Intercortical connections of corpus callosum as indicated by evoked potentials. *J. Neurophysiol.* 3 (5), 407–413.
- Dale, A.M., Fischl, B., Sereno, M.I., 1999. Cortical surface-based analysis. I. Segmentation and surface reconstruction. *NeuroImage* 9 (2), 179–194.
- Datta, A., Bansal, V., Diaz, J., Patel, J., Reato, D., Bikson, M., 2009. Gyri-precise head model of transcranial direct current stimulation: improved spatial focality using a ring electrode versus conventional rectangular pad. *Brain Stimul.* 2 (4), 201–207.
- Datta, A., Truong, D., Minhas, P., Parra, L.C., Bikson, M., 2012. Inter-individual variation during transcranial direct current stimulation and normalization of dose using MRI-derived computational models. *Front. Psychiatry* 3, 91.
- Desikan, R.S., Ségonne, F., Fischl, B., Quinn, B.T., Dickerson, B.C., Blacker, D., Buckner, R.L., Dale, A.M., Maguire, R.P., Hyman, B.T., Albert, M.S., Killiany, R.J., 2006. An automated labeling system for subdividing the human cerebral cortex on MRI scans into gyral based regions of interest. *NeuroImage* 31 (3), 968–980.
- Diekhoff, S., Uludağ, K., Sparing, R., Tittgemeyer, M., Cavusoglu, M., von Cramon, D.Y., Grefkes, C., 2011. Functional localization in the human brain: gradient-echo, spin-echo, and arterial spin-labeling fMRI compared with neuronavigated TMS. *Hum. Brain Mapp.* 32 (3), 341–357.
- Dmochowski, J.P., Datta, A., Bikson, M., Su, Y., Parra, L.C., 2011. Optimized multi-electrode stimulation increases focality and intensity at target. *J. Neural Eng.* 8 (4), 046011.
- Fischl, B., Dale, A.M., 2000. Measuring the thickness of the human cerebral cortex from magnetic resonance images. *Proc. Natl. Acad. Sci. U. S. A.* 97 (20), 11050–11055.
- Fischl, B., Sereno, M.I., Tootell, R.B., Dale, A.M., 1999. High-resolution intersubject averaging and a coordinate system for the cortical surface. *Hum. Brain Mapp.* 8 (4), 272–284.
- Fonov, V., Evans, A., McKinstry, R., Almlí, C., Collins, D., 2009. Unbiased nonlinear average age-appropriate brain templates from birth to adulthood. *NeuroImage. Organization for Human Brain Mapping 2009 Annual Meeting Vol. 47, Suppl. 1(0)*, p. S102.
- Fonov, V., Evans, A.C., Botteron, K., Almlí, C.R., McKinstry, R.C., Collins, D.L., Brain Development Cooperative Group, 2011. Unbiased average age-appropriate atlases for pediatric studies. *NeuroImage* 54 (1), 313–327.
- Francis, J.T., Gluckman, B.J., Schiff, S.J., 2003. Sensitivity of neurons to weak electric fields. *J. Neurosci.* 23 (19), 7255–7261.
- Fregni, F., Pascual-Leone, A., 2007. Technology insight: noninvasive brain stimulation in neurology – perspectives on the therapeutic potential of rTMS and tDCS. *Nat. Clin. Pract. Neurol.* 3 (7), 383–393.
- Freygang Jr., W., Landau, W.M., 1955. Some relations between resistivity and electrical activity in the cerebral cortex of the cat. *J. Cell. Physiol.* 45 (3), 377–392.
- Furubayashi, T., Terao, Y., Arai, N., Okabe, S., Mochizuki, H., Hanajima, R., Hamada, M., Yugeta, A., Inomata-Terada, S., Ugawa, Y., 2008. Short and long duration transcranial direct current stimulation (tDCS) over the human hand motor area. *Exp. Brain Res.* 185 (2), 279–286.
- Gabriel, S., Lau, R.W., Gabriel, C., 1996. The dielectric properties of biological tissues: II. Measurements in the frequency range 10 Hz to 20 GHz. *Phys. Med. Biol.* 41 (11), 2251–2269.
- Gabriel, C., Peyman, A., Grant, E.H., 2009. Electrical conductivity of tissue at frequencies below 1 MHz. *Phys. Med. Biol.* 54 (16), 4863–4878.
- Hauaeisen, J., Ramon, C., Eisele, M., Brauer, H., Nowak, H., 1997. Influence of tissue resistivities on neuromagnetic fields and electric potentials studied with a finite element model of the head. *IEEE Trans. Biomed. Eng.* 44 (8), 727–735.
- Ho, K.A., Taylor, J.L., Chew, T., Gálvez, V., Alonzo, A., Bai, S., Dokos, S., Loo, C.K., 2016. The effect of transcranial direct current stimulation (tDCS) electrode size and current intensity on motor cortical excitability: evidence from single and repeated sessions. *Brain Stimul.* 9 (1), 1–7. <http://dx.doi.org/10.1016/j.brs.2015.08.003>.
- Hummel, F.C., Celnik, P., Pascual-Leone, A., Fregni, F., Byblow, W.D., Buetefisch, C.M., Rothwell, J., Cohen, L.G., Gerloff, C., 2008. Controversy: noninvasive and invasive cortical stimulation show efficacy in treating stroke patients. *Brain Stimul.* 1 (4), 370–382.
- Johnson, H., Harris, G., Williams, K., 2007. BRAINSFit: mutual information registrations of whole-brain 3D images, using the Insight Toolkit. *Insight J.* <http://hdl.handle.net/1926/1291>.
- Jurcak, V., Tsuzuki, D., Dan, I., 2007. 10/20, 10/10, and 10/5 systems revisited: their validity as relative head-surface-based positioning systems. *NeuroImage* 34 (4), 1600–1611.
- Klein, A., Ghosh, S.S., Avants, B., Yeo, B.T.T., Fischl, B., Ardekani, B., Gee, J.C., Mann, J.J., Parsey, R.V., 2010. Evaluation of volume-based and surface-based brain image registration methods. *NeuroImage* 51 (1), 214–220.
- Kuo, H.L., Bikson, M., Datta, A., Minhas, P., Paulus, W., Kuo, M.F., Nitsche, M.A., 2013. Comparing cortical plasticity induced by conventional and high-definition 4 × 1 ring tDCS: a neurophysiological study. *Brain Stimul.* 6 (4), 644–648.
- Kuo, M.F., Paulus, W., Nitsche, M.A., 2014. Therapeutic effects of non-invasive brain stimulation with direct currents (tDCS) in neuropsychiatric diseases. *NeuroImage* 85 (Pt 3), 948–960.
- Laakso, I., Hirata, A., 2012. Fast multigrid-based computation of the induced electric field for transcranial magnetic stimulation. *Phys. Med. Biol.* 57 (23), 7753–7765.
- Laakso, I., Tanaka, S., Koyama, S., De Santis, V., Hirata, A., 2015. Inter-subject variability in electric fields of motor cortical tDCS. *Brain Stimul.* 8 (5), 906–913.
- Lang, N., Siebner, H.R., Ward, N.S., Lee, L., Nitsche, M.A., Paulus, W., Rothwell, J.C., Lemon, R.N., Frackowiak, R.S., 2005. How does transcranial DC stimulation of the primary motor cortex alter regional neuronal activity in the human brain? *Eur. J. Neurosci.* 22 (2), 495–504.
- Latikka, J., Kuurne, T., Eskola, H., 2001. Conductivity of living intracranial tissues. *Phys. Med. Biol.* 46 (6), 1611–1616.
- Lindenberger, R., Nachtigall, L., Meinzer, M., Sieg, M.M., Flöel, A., 2013. Differential effects of dual and unihemispheric motor cortex stimulation in older adults. *J. Neurosci.* 33 (21), 9176–9183.
- Lindenblatt, G., Silny, J., 2001. A model of the electrical volume conductor in the region of the eye in the ELF range. *Phys. Med. Biol.* 46 (11), 3051–3059.
- López-Alonso, V., Cheeran, B., Rio-Rodríguez, D., Fernández-Del-Olmo, M., 2014. Inter-individual variability in response to non-invasive brain stimulation paradigms. *Brain Stimul.* 7 (3), 372–380.
- López-Alonso, V., Fernández-Del-Olmo, M., Costantini, A., Gonzalez-Henriquez, J.J., Cheeran, B., 2015. Intra-individual variability in the response to anodal transcranial direct current stimulation. *Clin. Neurophysiol.*
- Marquez, J., van Vliet, P., McElduff, P., Lagopoulos, J., Parsons, M., 2015. Transcranial direct current stimulation (tDCS): does it have merit in stroke rehabilitation? A systematic review. *Int. J. Stroke* 10 (3), 306–316.
- Mehta, A.R., Pogossyan, A., Brown, P., Brittain, J.S., 2015. Montage matters: the influence of transcranial alternating current stimulation on human physiological tremor. *Brain Stimul.* 8 (2), 260–268.
- Meron, D., Hedger, N., Garner, M., Baldwin, D.S., 2015. Transcranial direct current stimulation (tDCS) in the treatment of depression: systematic review and meta-analysis of efficacy and tolerability. *Neurosci. Biobehav. Rev.* 57, 46–62.
- Minhas, P., Bansal, V., Patel, J., Ho, J.S., Diaz, J., Datta, A., Bikson, M., 2010. Electrodes for high-definition transcutaneous DC stimulation for applications in drug delivery and electrotherapy, including tDCS. *J. Neurosci. Methods* 190 (2), 188–197.
- Miranda, P.C., Mekonnen, A., Salvador, R., Ruffini, G., 2013. The electric field in the cortex during transcranial current stimulation. *NeuroImage* 70, 48–58.
- Moliadze, V., Antal, A., Paulus, W., 2010. Boosting brain excitability by transcranial high frequency stimulation in the ripple range. *J. Physiol.* 588 (24), 4891–4904.
- Nitsche, M.A., Paulus, W., 2000. Excitability changes induced in the human motor cortex by weak transcranial direct current stimulation. *J. Physiol. Lond.* 527 (Pt 3), 633–639.
- Nitsche, M.A., Paulus, W., 2001. Sustained excitability elevations induced by transcranial DC motor cortex stimulation in humans. *Neurology* 57 (10), 1899–1901.
- Nitsche, M.A., Doemkes, S., Karaköse, T., Antal, A., Liebetanz, D., Lang, N., Tergau, F., Paulus, W., 2007. Shaping the effects of transcranial direct current stimulation of the human motor cortex. *J. Neurophysiol.* 97 (4), 3109–3117.
- Nitsche, M.A., Cohen, L.G., Wassermann, E.M., Priori, A., Lang, N., Antal, A., Paulus, W., Hummel, F., Boggio, P.S., Fregni, F., Pascual-Leone, A., 2008. Transcranial direct current stimulation: state of the art 2008. *Brain Stimul.* 1 (3), 206–223.
- Opitz, A., Paulus, W., Will, S., Antunes, A., Thielscher, A., 2015. Determinants of the electric field during transcranial direct current stimulation. *NeuroImage* 109, 140–150.
- Polanía, R., Nitsche, M.A., Paulus, W., 2011a. Modulating functional connectivity patterns and topological functional organization of the human brain with transcranial direct current stimulation. *Hum. Brain Mapp.* 32 (8), 1236–1249.
- Polanía, R., Paulus, W., Antal, A., Nitsche, M.A., 2011b. Introducing graph theory to track for neuroplastic alterations in the resting human brain: a transcranial direct current stimulation study. *NeuroImage* 54 (3), 2287–2296.
- Priori, A., Berardelli, A., Rona, S., Accornero, N., Manfredi, M., 1998. Polarization of the human motor cortex through the scalp. *Neuroreport* 9 (10), 2257–2260.
- Rahman, A., Reato, D., Arlotti, M., Gasca, F., Datta, A., Parra, L.C., Bikson, M., 2013. Cellular effects of acute direct current stimulation: somatic and synaptic terminal effects. *J. Physiol.* 591 (10), 2563–2578.

- Ranck Jr., J., 1963. Specific impedance of rabbit cerebral cortex. *Exp. Neurol.* 7, 144–152.
- Ruffini, G., Fox, M.D., Ripolles, O., Miranda, P.C., Pascual-Leone, A., 2014. Optimization of multifocal transcranial current stimulation for weighted cortical pattern targeting from realistic modeling of electric fields. *NeuroImage* 89, 216–225.
- Sadleir, R., Vannorsdall, T.D., Schretlen, D.J., Gordon, B., 2012. Target optimization in tDCS. *Front. Psychiatry* 3, 90.
- Saturnino, G.B., Antunes, A., Thielscher, A., 2015. On the importance of electrode parameters for shaping electric field patterns generated by tDCS. *NeuroImage* 120, 25–35.
- Sehm, B., Kipping, J., Schäfer, A., Villringer, A., Ragert, P., 2013. A comparison between uni- and bilateral tDCS effects on functional connectivity of the human motor cortex. *Front. Hum. Neurosci.* 7, 183.
- Shahid, S.S., Bikson, M., Salman, H., Wen, P., Ahfock, T., 2014. The value and cost of complexity in predictive modelling: role of tissue anisotropic conductivity and fibre tracts in neuromodulation. *J. Neural Eng.* 11 (3), 036002.
- Sparing, R., Buelte, D., Meister, I.G., Paus, T., Fink, G.R., 2008. Transcranial magnetic stimulation and the challenge of coil placement: a comparison of conventional and stereotaxic neuronavigational strategies. *Hum. Brain Mapp.* 29 (1), 82–96.
- Stoy, R.D., Foster, K.R., Schwan, H.P., 1982. Dielectric properties of mammalian tissues from 0.1 to 100 MHz: a summary of recent data. *Phys. Med. Biol.* 27 (4), 501–513.
- Suh, H.S., Lee, W.H., Kim, T.S., 2012. Influence of anisotropic conductivity in the skull and white matter on transcranial direct current stimulation via an anatomically realistic finite element head model. *Phys. Med. Biol.* 57 (21), 6961–6980.
- Tanaka, S., Watanabe, K., 2009. Transcranial direct current stimulation – a new tool for human cognitive neuroscience. *Brain Nerve* 61 (1), 53–64.
- Tay, G., Chibbert, M., Battocletti, J., Sances Jr., A., Swiontek, T., Kurakami, C., 1989. Measurement of magnetically induced current density in saline in vivo in 'Engineering in Medicine and Biology Society, 1989'. *Images of the Twenty-First Century. Proceedings of the Annual International Conference of the IEEE Engineering*, pp. 1167–1168 (in'). (<http://ieeexplore.ieee.org/stamp/stamp.jsp?arnumber=96142>).
- Tremblay, S., Lepage, J.F., Latulipe-Loiselle, A., Fregni, F., Pascual-Leone, A., Théoret, H., 2014. The uncertain outcome of prefrontal tDCS. *Brain Stimul.* 7 (6), 773–783.
- Truong, D.Q., Magerowski, G., Blackburn, G.L., Bikson, M., Alonso-Alonso, M., 2013. Computational modeling of transcranial direct current stimulation (tDCS) in obesity: impact of head fat and dose guidelines. *NeuroImage Clin.* 2, 759–766.
- Van Essen, D.C., Dierker, D.L., 2007. Surface-based and probabilistic atlases of primate cerebral cortex. *Neuron* 56 (2), 209–225.
- Wagner, T., Zahn, M., Grodzinsky, A., Pascual-Leone, A., 2004. Three-dimensional head model simulation of transcranial magnetic stimulation. *IEEE Trans. Biomed. Eng.* 51 (9), 1586–1598.
- Wagner, S., Rampersad, S.M., Aydin, Ü., Vorwerk, J., Oostendorp, T.F., Neuling, T., Herrmann, C.S., Stegeman, D.F., Wolters, C.H., 2014. Investigation of tDCS volume conduction effects in a highly realistic head model. *J. Neural Eng.* 11 (1), 016002.
- Wiethoff, S., Hamada, M., Rothwell, J.C., 2014. Variability in response to transcranial direct current stimulation of the motor cortex. *Brain Stimul.* 7 (3), 468–475.
- Winkler, A.M., Sabuncu, M.R., Yeo, B.T.T., Fischl, B., Greve, D.N., Kochunov, P., Nichols, T.E., Blangero, J., Glahn, D.C., 2012. Measuring and comparing brain cortical surface area and other areal quantities. *NeuroImage* 61 (4), 1428–1443.
- Yeo, B.T.T., Sabuncu, M.R., Vercauteren, T., Ayache, N., Fischl, B., Golland, P., 2010. Spherical demons: fast diffeomorphic landmark-free surface registration. *IEEE Trans. Med. Imaging* 29 (3), 650–668.